Structure−Function Relationships in Side Chain Lactam Cross-Linked Peptide Models of a Conserved N-Terminal Domain of Apolipoprotein E†

Tammie L. S. Benzinger,‡ Demetrios T. Braddock,§,○ Samuel R. Dominguez,‡ Timothy S. Burkoth,|| Hélène Miller-Auer,‡ Ram M. Subramanian,‡ Gunther M. Fless,⊥ David N. M. Jones,§,▽ David G. Lynn,|| and Stephen C. Meredith*,‡

Departments of Chemistry, Biochemistry and Molecular Biology, Medicine, and Pathology, The University of Chicago, 5841 South Maryland Avenue, Chicago, Illinois 60637

Received March 2, 1998; Revised Manuscript Received July 2, 1998

ABSTRACT: Bioactive peptides have multiple conformations in solution but adopt well-defined conformations at lipid surfaces and in interactions with receptors. We have used side chain lactam cross-links to stabilize secondary structures in the following peptide models of a conserved N-terminal domain of apolipoprotein E (cross-link periodicity in parentheses): I, H_2N-GQTLSEQVQEELLSSQVTQELRAG-COOH (none); III, H_2N-GDTLKEQVQEELLSEQVKDELKAG-COOH (*i* to *i* + 3); IV, H_2N-GQDLSEKVQEELLESQVK-DELLKAG-COOH (*i* to *i* + 4); IVa, H_2N-GQDLSEKVQEELLSEQVKDELLKAG-COOH (*i* to *i* + 4) (lactams above the sequence, potential salt bridges below the sequence). We previously demonstrated [Luo et al. (1994) *Biochemistry 33*, 12367−12377; Braddock et al. (1996) *Biochemistry 35*, 13975−13984] that peptide III, containing lactam cross-links between the *i* and *i* + 3 side chains, enhances specific binding of LDL via a receptor other than the LDL-receptor. Peptide III in solution consists of two short α helices connected by a non α helical segment. Here we examine the hypothesis that the domain modeled by peptide III is one antipode of a conformational switch. To model another antipode of the switch, we introduced two strategic modifications into peptide III to examine structure−function relationships in this domain: (1) the spacing of the lactam cross-links was changed (*i* to *i* + 4 in peptides IV and IVa) and (2) peptides IV and IVa contain the two alternative sequences at a site of a possible end-capping interaction in peptide III. The structure of peptide IV, determined by 2D-NMR, is α helical across its entire length. Despite the remarkable degree of structural order, peptide IV is biologically inactive. In contrast, peptides III and possibly IVa contain a central interruption of the α helix, which appears necessary for biological activity. These and other studies support the hypothesis that this domain is a conformational switch which, to the extent that it models apolipoprotein E itself, may modulate interactions between apo E and its various receptors.

Bioactive peptides have multiple conformations in solution, but adopt well-defined conformations at lipid interfaces and in interactions with receptors. The selective introduction of side chain cross-links, such as lactam bridges, into a peptide sequence results in enhancement and stabilization of secondary structures such as the α helix (*1*−*9*). The lactam bridge possesses distinct advantages as a cross-linking strategy, including ease of synthesis with high yields using existing techniques of solid-phase synthesis (*3*, *7*, *10*), resistance to proteolysis, and insensitivity to the redox conditions in biological media.

We have used this procedure to delineate structure−function relationships in peptide models of a conserved N-terminal domain of apolipoprotein E. This domain, containing amino acids 41−60 of human apolipoprotein E, had no previously known function. We conducted structural studies by circular dichroic spectroscopy and two-dimensional NMR spectroscopy of a peptide of this native sequence (peptide I) and a model peptide (peptide III) with a very similar amino sequence and the incorporation of side chain lactam cross-links (*i* to *i* + 3 residues). These studies demonstrated that peptide III contains two short α helical segments linked by a central non α segment, possibly a turn (*9*). This structure was reminiscent of that observed in the crystal of the N-terminal thrombolytic fragment of human apo E3 (*11*).

In parallel with the structural studies, we demonstrated that both peptides I and III increase binding of LDL to cell surfaces, and this binding is mediated by a receptor that was neither the LDL-receptor nor the LDL-receptor related

† This work was supported by NIH Grant HL-15062, SCOR in Atherosclerosis (S.C.M.), NIH R21 RR12723 (D.G.L.), the Medical Scientist National Research Service Award, NIH/National Institute of General Medical Sciences Grant 5 T32 GM07281 (T.L.S.B., S.R.D.), and the Cardiovascular Pathology Training Grant (T.S.B., Grant 5 T32 HL07237).

* To whom correspondence should be addressed: telephone, 773-702-1267; fax, 773-702-3778; e-mail, scmeredi@midway.uchicago.edu.

‡ Department of Pathology.

§ Department of Biochemistry and Molecular Biology.

|| Department of Chemistry.

⊥ Department of Medicine.

○ Current address: NIH-NCI, Department of Pathology, Building 10, Room 2N212, 10 Center Drive, Bethesda, MD 20892-1516.

▽ Current address: Department of Pharmacology, University of Colorado Health Science Center, Campus Box C-236, 4200 East Ninth Ave., Denver, CO 80262.

S0006-2960(98)00482-6 CCC: $15.00
Published on Web 09/02/1998

protein (LRP; *10*). The lactam cross-linked peptide, moreover, was approximately 10-fold more active than the native peptide, indicating that the non-cross-linked peptide could also adopt conformations other than the bioactive one, while cross-linking constrained peptide III to adopt predominantly a bioactive conformation. These observations suggest that the domain modeled by peptides I and III might constitute a conformational switch domain, which might correspond to a similar switch in apo E itself. The existence of a switch domain in apo E is supported by the dramatic changes in LDL-receptor affinity which occurs as the protein is transferred from aqueous solution to an amphiphilic environment such as the lipid−water interface (*12*).

In this paper we will examine the hypothesis that the conserved domain modeled by peptides I and III is a switch domain. The bioactive peptide III may represent one antipode of the switch—one in which, to the extent that it models the situation in apo E itself, the protein would have a high affinity for a receptor other than the LDL-receptor or LRP. To model another antipode of the switch, we have introduced two strategic modifications of peptide III. First, we altered the spacing of lactam cross-links, i.e., between the *i* and *i* + 4 residues in peptide IV. Second, the central region of peptide III showed interruption of the α helix and raised the possibility of an end-capping interaction; hence, we synthesized and studied peptide IVa to examine this possibility. In this paper, we will show that cross-links between *i* and *i* + 4 residues, like those between *i* and *i* + 3 residues, stabilize the α helix. In fact, we will show that peptide IV is α helical over the entire length of the peptide, which, remarkably, is associated with loss of all biological activity despite this high degree of structural order. We will discuss the possibility that this continuous α helix represents another antipode of a switch domain.

MATERIALS AND METHODS

Peptide Synthesis, Purification, and Analysis. Methods for synthesis, cleavage from resin, purification, and analysis of side chain lactam cross-linked peptides have been given elsewhere in detail (*9*, *10*). Briefly, the peptide chain was elongated using tBOC chemistry, and N^{α}-tBoc, Asp O^{β}-Fmoc, and N^{α}-tBoc Lys N^{ϵ}-Fmoc were used for residues to be cross-linked. When the second member of the cross-link had been incorporated into the chain, the synthesizer was changed to FMOC chemistry and the side chains were deprotected, and coupled as described previously. Peptide chain elongation was continued after the synthesizer had been switched back to tBOC chemistry.

Cells. Detailed descriptions of these techniques have been given elsewhere (*10*). For most of the recent experiments, mouse embryonic fibroblast cell lines were used, obtained from Drs. Joachim Herz and Thomas E. Willnow (University of Texas Southwestern Medical Center, Dallas). These included wild type and LDL-receptor/LRP deficient cells ("double mutants"). In the experiments concerning the mouse embryonic fibroblasts, two different assays for LDL binding were used: first, the method of Goldstein et al. (*13*), using ^{125}I-labeled LDL; and second, the method of ref *14*, which measures binding of 3,3′-dioctadecylindocarboxycyanine-labeled LDL (DiI-LDL) by fluorescence spectroscopy. Unless otherwise specified, each data point was the average of triplicates.

Circular Dichroic Spectroscopy. The circular dichroic (CD) spectra of peptides I, III, IV, and IVa in buffer (0.02 M sodium phosphate, pH 7.00, 0.15 M NaCl) or 2,2,2-trifluoroethanol (TFE)/water (1/1,v/v) were recorded using a Jasco J-600 spectropolarimeter. Peptide concentrations were varied between 1 μM and 0.4 mM; concentrations were determined by amino acid analysis (*15*). The spectropolarimeter was calibrated periodically with a standard solution of camphorsulfonic acid-*d* as described previously (*16*). For analysis of denaturation curves, the temperature of peptide solutions in TFE/water (1/1, v/v) was increased in increments of 10 °C, and the solutions were allowed to reach thermal equilibrium for 1 h, after which the $[\theta]_{222}$ was constant. In some experiments, absence of hysteresis was confirmed by cooling rather than heating the samples. Helical content was calculated by the equation of Greenfield and Fasman (*17*), i.e., % helix = 100% × (($[\theta]_{208}$ + 4000)/−29000). The thermodynamic parameters ΔG, ΔH, and ΔS for the unfolding of the peptide IV and its linear analogue, peptide I, were obtained using a two-state model as a first approximation, as we have done previously for peptide III (*9*). Briefly, the equilibrium is modeled as occurring between a helical (H) and a "random coil" (C) form and K_{unfold} is the equilibrium constant for the unfolding reaction.

$$K_{\text{unfold}} = \text{C/H} = ([\theta]_{\text{exp}} - [\theta]_{\text{H}})/([\theta]_{\text{C}} - [\theta]_{\text{H}})$$

where $[\theta]_{\text{exp}}$ is the experimental molar ellipticity of the peptide solution and $[\theta]_{\text{H}}$ and $[\theta]_{\text{C}}$ are the molar ellipticities of the helical and coil forms of the peptide, respectively. Since $\Delta G^{\circ}_{\text{unfold}} = -RT \ln K_{\text{unfold}}$ and $\Delta G^{\circ} = \Delta H^{\circ} - T\Delta S^{\circ}$, $\ln K_{\text{unfold}} = -(\Delta H^{\circ}/RT) + (\Delta S^{\circ}/R)$, and the enthalpy and entropy of the unfolding reaction can be obtained from a van't Hoff plot of $\ln K_{\text{unfold}}$ vs $1/T$.

NMR Spectroscopy. NMR stock samples were prepared by dissolving 20 mg of peptide in 600 μL of 5 mM sodium phosphate buffer, pH 7.0, 50% (v/v) TFE-d_3 (99% enrichment). Lower concentrations of peptide (10 mg/mL, 7.5 mg/mL, 5 mg/mL, and 1 mg/mL) were prepared by diluting the concentrated stock samples into the same solvent system. For exchange experiments, the stock samples were lyophilized, redissolved in 50 μL of H_2O/50% TFE-d_3, diluted with 550 μL of D_2O/50% TFE-d_3, and immediately inserted into the spectrometer.

All NMR experiments were recorded on a Varian 500 MHZ spectrometer at 20 °C. Hypercomplex quadrature detection (*18*) was used to obtain pure-phase absorption mode double-quantum-filtered correlation spectroscopy (DQF-COSY) (*19*) and nuclear Overhauser effect spectroscopy (NOESY) (*20*) spectra. Phase-sensitive total correlation spectroscopy (TOCSY) spectra (*21*) were recorded with the use of the DIPSI-2 spin−lock pulse (*22*). Typical two-dimensional data were recorded with 128, 256, or 512 free induction decays (FIDs) of 2k data points, 32 scans per FID, a spectral width of 5000 Hz in both dimensions, and a recycle delay of 2 s, which included 1.5 s of continuous irradiation solvent suppression (presat). NOESY spectra were recorded at mixing times of 50, 100, 200, 300, and 350 ms. TOCSY spectra were recorded at mixing times of 50, 75, 100, and 120 ms. Data processing used the Felix software package (MSI, Inc.). Data were apodized with a sine bell shifted by 75° in F1 and by 90° in F2. Mild Lorentzian−Gaussian

apodization was applied in both dimensions. Data were zero filled to 4096 by 1024 points in F2 and F1, respectively, prior to Fourier transformation.

The $^3J_{\alpha N}$ coupling constants were measured using DQF-COSY spectra recorded in H_2O and extracted using the method of Kim and Prestegard (*23*). For the exchange experiments, 1D-NMR spectra at 20 °C were recorded at regular intervals immediately following the addition of D_2O. At a later date, TOCSY experiments were run on the same samples to confirm the identification of labile cross-peaks.

Structure Calculations and NMR Constraints. All structures were calculated using the simulated annealing protocol (*24*−*26*) implemented in X-PLOR (version 3.1) that had been slightly modified to use starting structures with randomized ϕ and ψ angles (*27*). The NMR constraint set was composed of 186 NOE-based distance constraints (75 intraresidue, 63 sequential, and 48 medium-range ($2 \leq |i - j| \leq 4$)), 12 dihedral angle constraints, and 6 constraints for 3 hydrogen bonds. NOE constraints were classified as strong (≤3 Å), medium (≤4 Å), or weak (≤6 Å). Multiplicity corrections of 0.5 were applied to methyl groups, as described by Fletcher et al. (*28*). Calculations used random starting coordinates, r^6 summation parameters for the NOE effective energy term, an initial temperature of 1000 °C, 48 000 high-temperature steps, and 24 000 low-temperature steps.

Analytical Ultracentrifugation. Sedimentation equilibrium experiments were performed using a Beckman Optima XLA ultracentrifuge interfaced to an IBM PS/2 model 55SX personal computer, an An-60 Ti four-place rotor, and analytical cells equipped with six-channel charcoal-filled centerpieces. Equilibrium ultracentrifugation was performed on peptide IV at a concentration of 0.52 mM in TFE/water (1/1,v/v). Partial specific volume was estimated from amino acid composition, and solvent density was measured directly by pycnometry.

RESULTS

Peptide Design. The sequences of peptides I, III, IV, and IVa are as follows:

	Peptide	Crosslink Periodicity
I.	H_2N-GQTLSEQVQEELLSSQVTQELRAG-COOH	none
III.	H_2N-GDTLKEQVQEELLSEQVKDELKAG-COOH	i to i + 3
IV.	H_2N-GQDLSEKVQEELLESQVKDELLKAG-COOH	i to i + 4
IVa	H_2N-GQDLSEKVQEELLSEQVKDELLKAG-COOH	i to i + 4

Peptide I contains amino acids 40−62 of human apolipoprotein E, plus a Gly spacer at each end. Peptide III is the bioactive peptide previously reported (*9*, *10*). Peptide IV was designed to contain side chain lactam cross-links between i and $i + 4$ residues (solid lines; potential salt bridges shown with dashed lines) while making minimal modification of the primary structure of peptides I and III. Thus, in peptide IV, the positioning of the hydrophobic residues, the chain length, and the net charge of amino acids 41−60 in apo E are all maintained. Peptide IV also closely resembles peptide III except for the spacing of the cross-links. Earlier work (*10*) showed that an additional peptide, peptide II, which contains cross-links between i and $i + 5$ residues, was neither structurally ordered nor biological active, and thus peptide II has not been included in the present study.

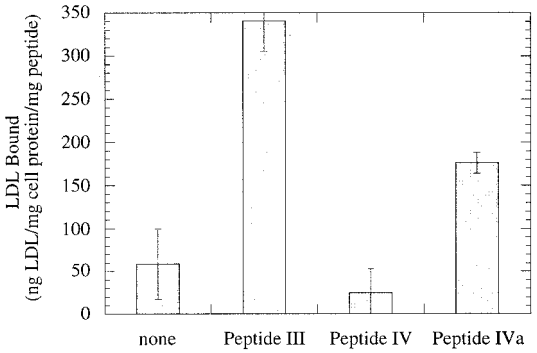

FIGURE 1: The binding of DiI-LDL to MEF4 cells in the presence or absence of peptides III, IV, or IVa. LDL was incubated with peptide or buffer for 1 h prior to addition to MEF4 cells under conditions described elsewhere (*10*). The quantity of LDL bound refers to specific binding as defined in essence by Goldstein et al. (*13*): i.e., the amount of DiI-LDL bound minus the amount of DiI-LDL bound in the presence of a 50-fold excess of unlabeled LDL. Similar results have been obtained using ^{125}I-LDL. Data points represent the mean of duplicate or triplicate samples; bars of the graph are the means ± standard deviation of 2−5 experiments. Data for peptide III represent both newly obtained values using DiI-LDL and older data adapted from Braddock et al. (*10*).

The central region of peptides III and IV differ from each other in that the order of the Ser14 and Glu15 in peptide III is reversed in peptide IV. The interruption of the α helix in the central region of peptide III raises the possibility of an end-capping effect, perhaps from the serine; accordingly we synthesized peptide IVa. Peptide IVa is identical to peptide IV, including the spacing of the cross-links, except that it reverses the order of the central Ser and Glu residues at positions 13 and 14, and in this one respect resembles peptide III.

Effect of Peptide IV on Binding of ^{125}I- or DiI-LDL to MEF1 and MEF4 Cells. Figure 1 shows the binding of LDL to MEF4 cells in the presence or absence of peptide III or IV (and peptide IVa). As shown previously, peptide III markedly increases the binding of LDL to these cells. In contrast, peptide IV does not show this biological activity at all. Since MEF4 cells do not have the LDL-receptor, there is reduced binding of LDL to these cells in the absence of peptides. In MEF1 cells, which do possess the LDL-receptor, however, peptide IV does not interfere with the interaction between LDL and the LDL-receptor (data not shown in graph).

Circular Dichroic Spectroscopy. In the two biologically active peptides, peptides I and III, the biological activity seems to correlate with the extent of α helical content (*9*, *10*). Peptide I is 15−20% α helical in TFE/water (1/1, v/v), while peptide III approaches 60% α helical. Since peptide IV is biologically inactive despite sequence homology to peptides I and III, it was of interest to know the α helical content of this peptide as well. In fact, as shown in Figure 2A, peptide IV, though biologically inactive, is more α-helical than even peptide III in aqueous buffers or in TFE/H_2O (1/1, v/v).

To compare the stabilization of α helicity in peptide IV to that in peptide III, thermal denaturation studies were performed; from the CD curves at various temperatures, van't

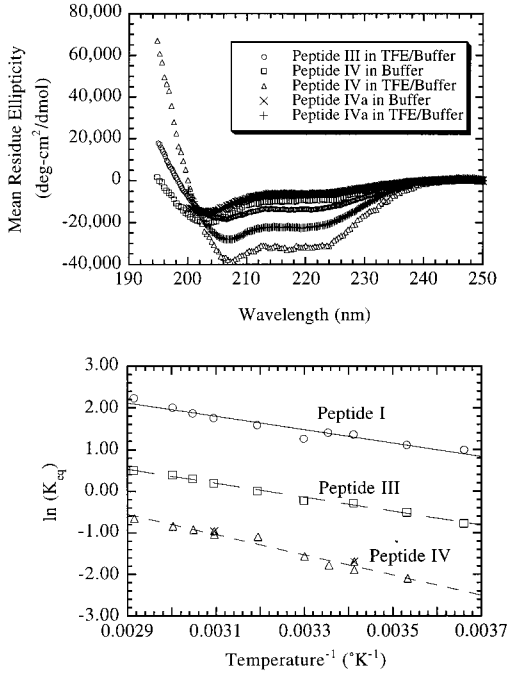

FIGURE 2: CD spectra and van't Hoff plot of thermal denaturation of peptide IV. Top, A: CD spectra of peptide IV and IVa in aqueous buffer and in TFE/water mixtures. Peptides were dissolved in either phosphate buffer (pH 7.00) or TFE/buffer mixtures from 10 to 50% (v/v) TFE. Spectra were collected and analyzed as described in Methods. Results shown represent the average of 3−10 scans. Bottom, B: van't Hoff plot of thermal denaturation of peptide IV. Experimental results for peptides I and III were first given in Luo et al. (*9*) and are reproduced here for comparison with peptide IV. A period of at least 1 h was allowed for thermal equilibration; thermal equilibration was assessed by monitoring the $[\theta]$ over time at each temperature (○, □, △ for peptides I, III, and IV, respectively). The denaturation was modeled as a two-step process between a helical (H) and coil (C) state; percent helicity was calculated according to the equation of Greenfield and Fasman (*19*). To demonstrate reversibility of the process, in some experiments the samples were first heated and then recooled to a given temperature (×). As in A, data points are from 3 to 10 scans; lines represent least-squares fit of the data to the equations $\Delta G°_{\text{unfold}} = RT \ln K_{\text{unfold}}$, $\Delta G° = \Delta H° - T\Delta S°$, and $\ln K_{\text{unfold}} = -(\Delta H°/RT) + (\Delta S°/R)$. For peptide I, the equation is $Y = -1611.6X + 6.795$ ($r = 0.969$). For peptide III, the equation is $Y = -1.677.7X + 5.391$ ($r = 0.995$). For peptide IV, the equation is $Y = -2435.4X + 6.507$ ($r = 0.984$).

Hoff plots were constructed for peptides I, III, and IV (Figure 2B). The lines for peptide I and IV differ in both slope and intercept, with the overall stabilization of peptide IV being 2 kcal/mol over that of peptide I. This is in contrast to peptide III, which gives a line in the van't Hoff plot parallel to the line for peptide I. We have previously proposed that the stabilization of peptide III is entirely attributable to a loss of entropy of the unfolded state of the peptide. In contrast, the van't Hoff plot for peptide IV shows an enthalpic as well as entropic contribution to the enhanced stability. These results are consonant with the CD data above, showing that peptide IV is essentially 100% α helical, whereas peptide III is only ≈60% helical. Denaturation of peptide IV therefore would involve the breaking of a greater number of hydrogen bonds than denaturation of peptide III.

NMR Resonance Assignments and Secondary Structure Analysis. Complete assignment of proton resonances for peptide IV were obtained using the standard assignment strategy of Wüthrich (*29*). Amino acid spin systems were primarily identified from the TOCSY cross-peak patterns (Figure 3). The two Val residues were distinctly identified by their double methyl resonances. The single Ala was uniquely identified by its single methyl resonance. The Gly was clearly identified by its single resonance. The Glu and Gln residues could be grouped by their multiple resonances between 2 and 3 ppm. Using the amide-amide region of the NOESY (Figure 4), where strong i to $i + 1$ connections were found for the entire sequence between residues 4 and

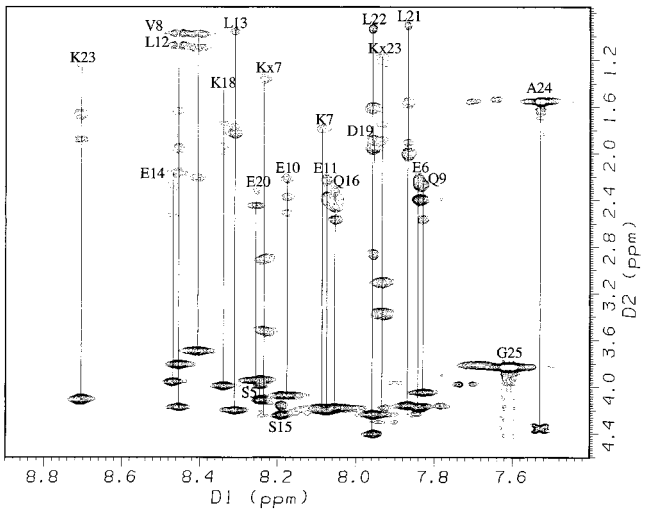

FIGURE 3: Amide to aliphatic region of the TOCSY spectrum of peptide IV. peptide IV was dissolved in TFE/water, at pH 7, using the procedure described in Methods. Spectra were acquired at 20 °C. Phase-sensitive TOCSY spectra with mixing times of 50, 75, 100, and 120 ms (*21*) were recorded with the use of the DIPSI-2 spin−lock pulse; shown is the 75 ms experiment. The intraresidue spin systems are each connected by a solid line and annotated by position in the sequence.

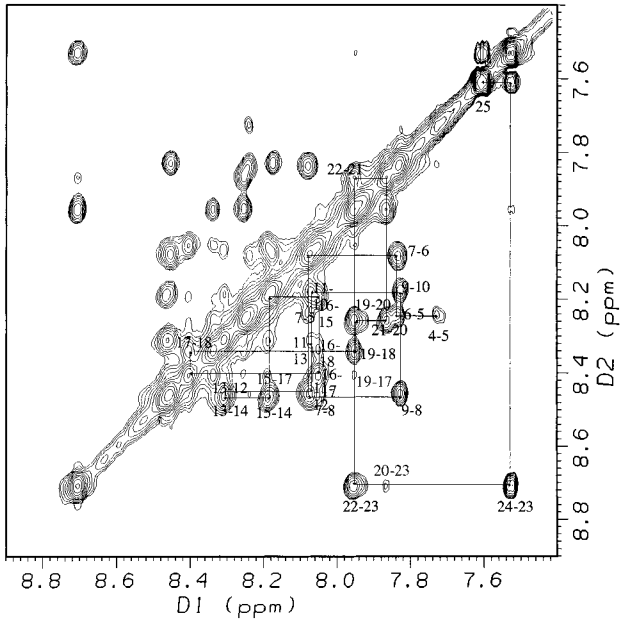

FIGURE 4: Amide−amide region of NOESY spectrum of peptide IV. NOESY spectra were acquired on a Varian 500 MHz spectrometer using mixing times of 50, 100, 150, 300, and 350 ms. The figure shows the NOESY spectrum obtained using 300 ms mixing time, with amide−amide cross-peaks visible across residues 4−25 of the peptide, including several i to $i + 2$ connections.

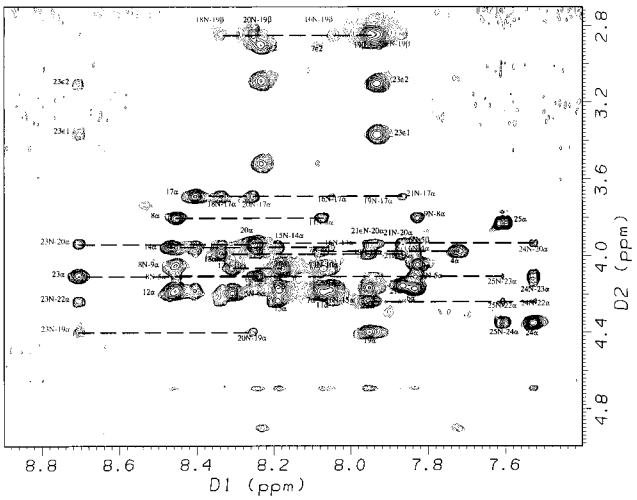

FIGURE 5: Amide−α region of the NOESY spectrum. The figure shows the amide (NH) to α ($C_\alpha H$) region of the NOESY spectrum, obtained using a mixing time of 300 ms. Intraresidue and sequential contacts are labeled by residue number. Further contacts (*i* to *i* + 3 and *i* to *i* + 4) are connected by dashed lines.

Table 1

residue	NH	$C_\alpha H$	$C_\beta H$	$C_\gamma H$	$C_\delta H$	$C_\epsilon H$; $N_\epsilon H$
D3 (x−K7)						
L4	7.73	3.97	1.78			
S5	8.24	4.11	3.99			
E6	7.84	4.17	2.26	2.39		
K7 (x−D3)	8.07	4.20	1.75	1.36	1.52	3.52, 2.91; 8.23
V8	8.45	3.80	1.98, 2.17	1.07, 0.96		
Q9	7.83	4.04	2.26	2.57		
E10	8.18	4.07	2.51, 2.37	2.21		
E11	8.07	4.20	2.22	2.39		
L12	8.45	4.17	1.95, 1.85			
L13	8.31	4.20	1.83, 1.76		0.96	
E14	8.47	3.96	2.28	2.53		
S15	8.19	4.24	4.16			
Q16	8.06	4.18	2.39, 2.46	2.56		
V17	8.40	3.69	2.21	1.09, 0.98		
K18	8.34	3.99	1.96	1.44	1.74	
D19 (x−K23)	7.955	4.40	2.87			
E20	8.25	3.94	2.45, 2.33	2.21		
L21	7.87	4.15	1.90, 2.00	1.57	0.91	
L22	7.96	4.23	1.95	1.60	0.93	
K23 (x−D19)	8.71	4.10	1.87	1.24	1.75, 1.65	3.37, 3.11; 7.93
A24	7.53	4.35	1.55			
G25	7.61	3.83				

25, combined with the TOCSY data, sequential assignment was relatively straightforward. The continuous *i* to *i* + 1 and additional *i* to *i* + 2 amide-amide connectivities are consistent with a highly ordered helical structure, in contrast to peptide III which had three separate discontinuities across the central region of the peptide. Additional NMR evidence supporting a continuous α helical structure for peptide IV was found in the amide (NH) to α ($C_\alpha H$) fingerprint region of the NOESY spectra (Figure 5), where strong *i* to *i* + 3 connectivities were seen across the entire peptide. From the DQF-COSY experiment, all of the $^3J_{\alpha N}$ coupling constants that could be measured were consistent with an α helical structure; those which could not be measured were obscured due to overlap with other residues.

For the exchange experiments, the peptide was first dissolved in 50 μL of H_2O/TFE and then diluted by adding 500 μL of D_2O/TFE. By using this procedure, we were able to observe all of the amide proton resonances, even the rapidly exchanging ones. Furthermore, the small amount of residual proton signal allowed us to perform a TOCSY experiment to identify the peaks in the equilibrated sample. The small pH difference (0.3) between the samples in H_2O and D_2O resulted in small chemical shift changes (0.05 ppm), which rendered unambiguous assignment impossible without the additional TOCSY experiment. All of the amide protons of peptide IV exchanged more slowly than those of non-cross-linked and less α helical peptides such as peptide I. However, only three of these protons had not completely equilibrated after several hours, and for the purpose of H-bond constraints, only these were classified as slowly exchanging. The NOESY assignments, coupling constant, and exchange data are summarized in Tables 1 and 2.

Table 2: Summary of NOE Connectivities

*α Helical defined as $^3J_{\alpha N} < 6$ Hz.

Determination of the Three-Dimensional Structure of Peptide IV. The NMR solution structure of peptide IV was calculated from the NOESY, $^3J_{\alpha N}$, and H-bond constraints, as described in Methods. Thirty structures are shown in Figure 6A; the backbone (C, C_α, N, NH) root-mean-square distance (RMSD) for residues 5−25 in these 30 structures is 2.02 Å. This is in contrast to Peptide III, (Figure 6B), where for three structures (out of 10) the backbone RMSD was 3.5 Å (*9*), generated primarily by diversity within the central non α helical region.

To ensure that the helical rigidity of peptide IV was not an artifact of any single input parameter, various simulated annealing conditions were compared, including initial structures with random vs helical conformations, exclusion of some or all of the $^3J_{\alpha N}$ coupling constants, lower starting temperatures, and fewer energy minimization steps. However, under each of these conditions, the helix passing through the central portion of the peptide was unaltered. Greater variability was seen in the amino terminus of the peptide, where there were fewer constraints; these residues (*1*−*4*) were therefore excluded from the final analysis of the peptide structure. In contrast, when peptide III was reexamined using similar tests, the helices at the N- and C-termini of the peptide remained relatively constant, but the central bend fluctuated wildly, demonstrating, once again, that peptides III and IV differ most significantly with respect to the flexibility of this central region.

Lack of Self-Association of Peptide IV. An unusual feature of the NMR data shown above is the 10−12 Hz line width

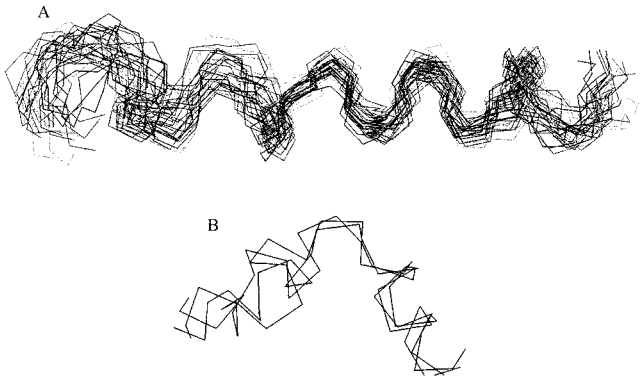

FIGURE 6: Three-dimensional structure of peptide IV. The NOE constraints, $^3J_{\alpha N}$ constraints and H-bond constraints, as summarized in Table 2, for peptide IV were used for simulated annealing calculations using X-PLOR. NOE constraints were classified as strong (≤3 Å), medium (≤4 Å), or weak (≤6 Å) based upon comparison of sequential NOESY experiments at various mixing times (50, 100, 200, 300, and 350 ms). Fifty structures were calculated, beginning from random coordinates as the starting geometry. Panel A shows the 30 lowest energy structures, for which the backbone RMSD (residues 5−25) is 2.02 Å. For comparison, three structures (of 10) generated for peptide III (*9*) by dynamic simulated annealing are shown in panel B and have a backbone RMSD of 3.5 Å.

of the amide protons. A similar phenomenon was observed for peptide III. One of the possibilities considered, but excluded experimentally, for peptide III was that the slow amide proton exchange was due to self-association. For peptide III, four independent lines of evidence demonstrated that peptide III was monomeric under all conditions studied: gel filtration chromatography, lack of peptide concentration dependence of specific ellipticity in CD spectroscopy, lack of change of line width with concentration in 1D-NMR experiments, and finally, the ultimate proof, analytical ultracentrifugation. Nevertheless, in the case of peptide IV, there was a more generalized slowing of amide proton exchange across the sequence, so it was again of interest to determine whether peptide IV self-associates. Peptide IV, like peptide III, did not show self-association by gel filtration chromatography, nor did it show concentration dependence of specific ellipticity in CD spectroscopy or change of line width with concentration or temperature in 1D-NMR experiments. To demonstrate definitively that peptide IV did not self-associate under the conditions used for NMR spectroscopy, we performed analytical ultracentrifugation (equilibrium sedimentation). By analytical sedimentation equilibrium ultracentrifugation of the peptide in phosphate buffer, pH 7.4, or in TFE/water (1/1, v/v), the molecular weight was 2730 (calculated MW = 2651).

Biological Activity and CD Spectroscopy of Peptide IVa. To examine the possibility of an end-capping interaction and to examine further the relationship between spacing of the cross-links and biological function in these model peptides, we performed LDL binding assays and CD spectroscopy for peptide IVa. As shown in Figure 1, unlike peptide IV, peptide IVa was biologically active. These experiments demonstrate that both the i to $i + 3$ cross-link spacing of peptide III and the i to $i + 4$ cross-link spacing of peptide IVa are compatible with biological activity. The CD spectra of peptide IVa are shown in Figure 2A. Peptide IVa has a CD spectrum similar to that of peptide III—that is, the helix content is 62% in TFE/H_2O (v/v = 1/1), compatible with a significant non α helical segment. These results support the hypothesis of a structure−function relationship. The CD spectrum of peptide IV is consonant with the NMR data and shows essentially 100% α helical content, and this is associated with the absence of biological activity. In contrast, peptides III and IVa have ≈60% α helical content which, in the case of peptide III, is found in two short helical segments. Both of these peptides have similar biological activity, though that of peptide III is greater than that of peptide IVa.

DISCUSSION

In this paper we used two-dimensional NMR spectroscopy and other techniques to study peptide IV, a model for apolipoprotein E residues 41−60, containing side chain lactam cross-links between i and $i + 4$ residues. Thermal denaturation studies showed that the α helix of peptide IV is more stable than that of peptide I by ≈2 kcal/mol and also more stable than that of peptide III by ≈1 kcal/mol. However, whereas the stabilization of peptide III is entirely attributable to loss of entropy of the unfolded state, the stabilization of peptide IV has both entropic and enthalpic components. The entropic stabilization is of quite similar magnitude to that observed for peptide III, suggesting that the two types of cross-links—i to $i + 3$ for peptide III and i to $i + 4$ for peptide IV—are equivalent. The enthalpic stabilization of peptide IV compared to peptides I and III can be attributed to that fact that peptide IV is entirely α helical, and thus denaturation of peptide IV requires the loss of a greater number of intrapeptide hydrogen bonds.

Despite its similarity to a biologically active peptide, peptide III and the less potent but still biologically active Peptide I (containing the native sequence of apo E residues 40−61), Peptide IV is biologically inactive in our assays of LDL binding. Peptides III and IV are similar not only in sequence but even in much of their three-dimensional structures. As shown by 2D-NMR, the only significant difference is that peptide IV has a continuous α helix while the two helices of peptide III are interrupted in the center of the peptide. In the minimization of the structures of peptide III, the central region was the most flexible and, hence, least clearly defined structure. The most straightforward interpretation of the difference in biological activity between peptides III and IV is that the disruption of α helix in the center of the peptide and the formation of another structure occurs in peptide III, but not peptide IV, and this is critical for biological activity. In support of this hypothesis, peptide IVa, which has a CD spectrum like that of peptide III, is biologically active. Although we have not determined the three-dimensional structure of peptide IVa, it is tempting to speculate that its structure resembles that of peptide III.

The question then arises as to why the α helix is disrupted in peptide III (and possibly also peptide IVa), but is continuous in peptide IV. It has been proposed (*30*−*33*) that the typical short length (≈12 amino acids) of α helices in proteins is attributable to certain consensus sequences that "end-cap", i.e., serve as boundary conditions for α helices. Previous data (*9*) was consistent with the occurrence of an end-capping interaction, possibly involving the Ser14 of peptide III. Ser is found in the same position of peptide

IVa, while in peptide IV, the Ser is at position 15. It is possible that an end-capping interaction might occur in peptides III and IVa, but not in peptide IV.

A much more definitive structure was obtained for peptide IV than for peptide III due to both the higher degree of order in the former peptide and several improvements in spectroscopy and data analysis. Thus, more than twice the number of constraints were available for determining the structure of peptide IV as were available for peptide III. Accordingly, the RMSD values for the 30 structures generated for peptide IV were considerably lower than that of the 10 structures generated for peptide III: backbone RMSD of 2.02 Å for 30 generated structures, as compared with backbone RMSD of 3.5 Å for 3 of 10 structures for peptide III. Except for the four residues at the amino terminus of peptide IV, this peptide appears to have a well-defined α helical structure with limited flexibility. The rigidity of this peptide is to be expected in the vicinity of the cross-links but is present even in the center of the peptide where there are no cross-links. In contrast, the central region of peptide III is less clearly defined. Although previously it was proposed that this region may contain a turn, the lack of spectroscopic precision precluded the assignment of any canonical structure to the region. Furthermore, the central domain of peptide III is probably more mobile than the corresponding region of peptide IV, meaning that the structure is inherently less well defined in the former case.

An unusual feature of peptide IV is the generally slow exchange of amide protons with solvent. A priori, it was possible that the slow exchange was due to shielding of the protons from solvent in a peptide aggregate. This possibility, however, was excluded by the demonstration, in sedimentation equilibrium experiments, that the peptide is monomeric under the same conditions as were used in the NMR experiments. It seems likely, therefore, that another explanation is needed. In view of the rigidity and high degree of order in the structure, it is possible that these protons exchange slowly with solvent because they are constrained to remain in intrapeptide hydrogen bonds. In other words, whereas the amide protons of a less ordered peptide (like peptide I) are relatively free to interact with either peptide or solvent alike, intrapeptide interactions are favored for the amide protons of peptide IV, resulting in slower exchange with solvent.

The studies presented above may shed light upon the structure and function of the N-terminal domain of apolipoprotein E. Apolipoprotein E is believed to undergo conformational changes as it is transferred between an isotropic solution and an amphiphilic environment such as the air−water or lipid−water interface. These conformational changes are believed to be associated with dramatic (500-fold) changes in affinity for the LDL-receptor. In our previous studies, we have shown that peptides of the highly conserved sequence itself and, a fortiori, specific models of this domain affect the interactions between LDL and another receptor which is neither the LDL-receptor nor the LRP. Taken together, these studies suggest the existence of a switch domain in apolipoprotein E—i.e., one that is capable of adopting more than one stable secondary or tertiary structure. The studies described in this paper demonstrate that rather minor sequence changes in this domain can have profound effects upon the three-dimensional structure and biological activities of this peptide. The central domain of peptides I, III, IV, and IVa appears capable of adopting either an α helical structure as in peptide IV, or a non-α helical structure as in peptide III and perhaps peptide IVa. In unpublished data, we have obtained evidence that peptide I is far more flexible than any of these other peptides, and can adopt all of the above structures. To the extent that these peptide models reflect the corresponding domain of apolipoprotein E itself, the conformational dynamics of these peptides may shed light on a hinge or switch region critical for interactions between multiple lipoproteins and their multiple receptors.

REFERENCES

1. Marqusee, S., and Baldwin, R. L. (1987) *Proc. Natl. Acad. Sci.* (*U.S.A.*) *84*, 8898−8902.
2. Oas, T. G., and Kim, P. S. (1988) *Nature 336*, 42−48.
3. Felix, A. M., Wang, C.-T., Heimer, E. P., and Fournier, A. (1988) *Int. J. Prot. Pept. Res. 31*, 231−238.
4. Pease, J. H., Storrs, R. W., and Wemmer, D. E. (1990) *Proc. Natl. Acad. Sci. U.S.A. 87*, 5643−5647.
5. Ruan, F., Chen, Y., and Hopkins, P. B. (1990) *J. Am. Chem. Soc. 112*, 9403−9404.
6. Ghadiri, M. R., and Fernholtz, A. K. (1990) *J. Am. Chem. Soc. 112*, 9633−9635.
7. Ösapay, G., and Taylor, J. W. (1992) *J. Am. Chem. Soc. 114*, 6966−6973.
8. Jackson, D. Y., King, D. S., Chmielewski, J., Singh, S., and Schultz, P. G. (1991) *J. Am. Chem. Soc. 113*, 9391−9392.
9. Luo, P.-Z., Braddock, D. T., Meredith, S. C., and Lynn, D. (1994) *Biochemistry 33*, 12367−12377.
10. Braddock, D. T., Mercurius, K. O., Subramanian, R. M., Dominguez, S. R., Davies, P. F., and Meredith, S. C. (1996) *Biochemistry 35*, 13975−13984.
11. Wilson, C., Wardell, M. R., Weisgraber, K. H., Mahley, R. W., and Agard, D. A. (1991) *Science 252*, 1817−1822.
12. Westerlund, J. A., and Weisgraber, K. H. (1993) *J. Biol. Chem. 268*, 15745−50.
13. Goldstein, J. L., Basu, S. K., and Brown, M. S. (1983) *Methods Enzymol. 98*, 241−260.
14. Stephan, Z. F., and Yurachek, E. C. (1993) *J. Lipid Res. 34*, 325−330.
15. Heinrikson, R. L. and Meredith, S. C. (1984) *Anal. Biochem. 136*, 65−74.
16. Nakagawa, Y., Gillen M. F., and Williams R. E. (1976) *Can. J. Chem. 54*, 3200−3202.
17. Greenfield N., and Fasman G. D. (1969) *Biochemistry 8*, 4108−4116.
18. States, D. J., Haberkorn, R. A., and Ruben, D. J. (1982) *J. Magn. Res. 48*, 286−292.
19. Rance, M., Srenson, O. W., Bodenhausen, G., Wagner, G., Ernst, R. R., and Wüthrich, K. (1983) *Biochem. Biophys. Res. Commun. 117*, 479−485.
20. Macura, S., and Ernst, R. R. (1980) *Mol. Phys. 41*, 95−117.
21. Bax, A., and Davis, D. G. (1985) *J. Magn. Res. 65*, 355−360.
22. Shaka, A. J., Lee, C. J., and Pines, A. (1988) *J. Magn. Reson. 77*, 274−293.
23. Kim, Y., and Prestegard, J. H. (1989) *J. Magn. Res. 84*, 9−13.
24. Nilges, M., Gronenborn, A. M., Brünger, A. T., and Clore, G. M. (1988) *Protein Eng. 2*, 27−38.
25. Nilges, M., Kuszewski, J., and Brünger, A. T. (1991) In *Computational Aspects of the Study of Biological Macromolecules by NMR* (Hoch, J. C., Poulsen, F. M., and Redfield, C., Eds.) Plenum Press, New York.

26. Brünger, A. T. (1992) X-PLOR Version 3.1: A System for Crystallography and NMR, Yale University, New Haven, CT.
27. Jones, D. N. M., Searles, M. A., Shaw, G. L., Churchill, M. E. A., Ner, S. S., Keeler, J., Travers, A. A., and Neuhaus, D. (1994) *Structure 2*, 609−627.
28. Fletcher, C. M., Jones, D. N. M., Diamond, R., and Neuhaus, D. (1996) *J. Biomol. NMR 8*, 292−310.
29. Wüthrich, K. (1986) *NMR of Proteins and Nucleic Acids*, John Wiley and Sons, New York.
30. Presta, L. G., and Rose, G. D. (1988) *Science 240*, 1632−1641.
31. Richardson, J. S., and Richardson, D. C. (1988) *Science 240*, 1648−1652.
32. Stickle, D. F., Presta L. G., Dill, K. A., and Rose, G. D. (1992), *J. Mol. Biol. 226*, 1143−1159.
33. Harper, E. T., and Rose, G. D. (1993) *Biochemistry 32*, 7605−7609.

BI980482F